Histol Histopathol (2023) 38: 1157-1168

Histology and Histopathology
From Cell Biology to Tissue Engineering

ORIGINAL ARTICLE Open Access

MiR-196a-5p facilitates progression of estrogen-dependent endometrial cancer by regulating FOXO1

Yuzhang Zhu[1], Yanfei Tang[2], Yaohua Fan[1] and Dongjuan Wu[1]

[1]Department of Oncology and [2]Department of Pediatrics, The Second Affiliated Hospital of Jiaxing University, Jiaxing Second Hospital, Jiaxing, Zhejiang, China

Summary. Background and Purpose. Estrogen-dependent endometrial cancer mainly occurs in younger pre-menopausal and post-menopausal women and threatens their health. Recently, microRNAs (miRNAs) have been considered as novel targets in endometrial cancer treatment. Therefore, we aimed to explore the effect of miRNA (miR)-196a-5p in estrogen-dependent endometrial cancer.

Methods. 17β-estradiol (E2; 2.5, 5, 10 and 20 nM) was used to treat RL95-2, HEC-1B and ECC-1 cells followed by cell viability assessment using 3-(4,5-dimethylthiazol-2-yl)-2,5-diphenyltetrazolium bromide (MTT). The level of miR-196a-5p was measured by reverse transcription-quantitative PCR (RT-qPCR). We then transfected miR-196a-5p mimic/inhibitor and Forkhead box protein O1 (FOXO1) small interfering RNA (siRNA) into E2-treated cells. Apoptotic cells were measured by flow cytometry. Wound healing and Transwell assays were implemented to assess migration and invasion. Bioinformatics and luciferase reporter assays were applied to confirm the interaction between miR-196a-5p and FOXO1. Immunoblotting determined the levels of FOXO1, Bcl-2, Bax, Caspase 3.

Results. E2 promoted cell viability and miR-196a-5p expression in RL95-2 and ECC-1 cells. miR-196a-5p mimic enhanced cell viability, migration and invasion but suppressed apoptosis and FOXO1, whilst miR-196a-5p inhibitor blocked these processes. In addition, miR-196a-5p upregulated Bcl-2, but down regulated Bax and Caspase 3 expression, an effect that was reversed by miR-196a-5p inhibitor. We determined that miR-196a-5p targeted FOXO1, and that si-FOXO1 blocked the effects of miR-196a-5p inhibitor on viability, apoptosis, migration and invasion of E2-treated RL95-2 and ECC-1 cells.

Conclusions. Our findings suggested potential diagnostic and therapeutic applications for miR-196a-5p and its FOXO1 target in patients suffering from estrogen-dependent endometrial cancer.

Key words: microRNA-196a-5p, Estrogen, Endometrial cancer, Forkhead box protein O1

Corresponding Author: Dongjuan Wu, Department of Oncology, The Second Affiliated Hospital of Jiaxing University, 1518, Huancheng North Road, Nanhu District, Jiaxing City, Zhejiang Province, 314000, China. e-mail: wudongjuanmrs@163.com

www.hh.um.es. DOI: 10.14670/HH-18-572

Introduction

Endometrial cancer, an epithelial carcinoma which primarily occurs in the endometrium, is one of the most common cancers in women and accounts for 76,000 deaths yearly among women worldwide (Morice et al., 2016). Based on the traditional classification, endometrial cancer is subdivided into type I and type II tumors (Chen et al., 2018). Type I tumor is commonly an endometrioid type which is associated with long-term endometrial hyperplasia or aberrant glandular proliferation (Bokhman, 1983), and accounts for more than 80% of cases (Doll et al., 2008). In addition, the type I tumor is estrogen-dependent and its established risk factors are prolonged exposure to estrogen without progesterone antagonism, obesity, diabetes, nulliparity, early menarche and late menopause (Setiawan et al., 2013) It has been reported that estrogen-dependent endometrial cancer predominately arises in younger pre-menopausal and post-menopausal women and threatens their health (Zhou et al., 2021). Therefore, exploring the pathogenesis of estrogen-dependent endometrial cancer and finding specific markers has important clinical significance for its early diagnosis and treatment.

MicroRNAs (miRNAs) have been shown to modulate gene expression through target gene regulation (Pu et al., 2019). Abnormal miRNAs have been observed in many tumors, resulting in dysfunction of cell cycle, survival and differentiation (Wang et al., 2020). Some miRNAs were reported to serve as oncogenes that promote tumorigenesis and progression, including miR-182-5p (Hirata et al., 2012) and miR-31 (Liu et al., 2010) , while others such as miR-34b (Lee et al., 2011) and miR-7 (Kong et al., 2012) function as

tumor suppressors. Compelling evidence indicates that miRNA expression may provide potential and minimally invasive biomarkers for diagnosis and management of carcinoma (Banno et al., 2014). A recent study identified miR-196a-5p as overexpressed in gastric cancer cells and showed that its inhibition reversed epithelial-mesenchymal transition and invasion through targeting Smad4 (Pan et al., 2017). Furthermore, miR-196a has been reported to function as an oncogene by promoting cell proliferation and stimulating cell cycle transition (Hou et al., 2014). Nevertheless, the function of miR-196a-5p in estrogen-dependent endometrial cancer is still poorly understood.

Previous studies have shown that FOXO1 knockdown promotes the proliferative capacity of endometrial cancer cells and inhibits apoptosis (Yan et al., 2021). However, whether miR-196a-5p is involved in the progression of estrogen-dependent endometrial cancer by regulating FOXO1 remains unclear. In this study, the related mechanism experiments confirmed that FOXO1 was one of the target genes of MIR-196a-5p. Further studies showed that MIR-196a-5p promotes E2-induced cell proliferation, migration, proliferation and invasion, and inhibited cell apoptosis by targeting FOXO1, thereby promoting estrogen-dependent endometrial carcinoma. These findings reveal the potential function of miR-196a-5p and suggest that miR-196a-5p may be an important diagnostic, therapeutic and prognostic biomarker for endometrial cancer.

Materials and methods

Cell culture

The human endometrial cancer cell line RL95-2, HEC-1B and ECC-1 cells were provided by American Type Culture Collection (ATCC, Rockville, MD, USA). Cells were maintained in RPMI-1640 medium (Gibco, USA) containing 10% fetal bovine serum and 100 units/mL penicillin/streptomycin at 37°C under 5% CO_2. Cells were passaged and the fourth generation was collected.

E2 (HAS Biotech, China) was dissolved in dimethyl sulfoxide (DMSO, Sigma-Aldrich, USA) and different concentrations of E2 (2.5, 5, 10 and 20 nM) were applied to RL95-2, HEC-1B and ECC-1 cells for 48h at 37°C. Cells treated with DMSO alone served as controls.

Cell transfectiong

E2-treated RL95-2 and ECC-1 cells (1×10^6 cells/well) were incubated in 6-well plates (Corning, USA) at 37°C. When cells reached 60-80% confluency, 100 nM of miR-196a-5p mimics (sense: 5'-UAGGU AGUUUCAUGUUGUUGGG-3' and anti-sense: 5'-CCCAACAACAUGAAACUACCUA-3') or mimic negative control (NC; sense: 5'-UUCUCCGAACGU GUCACGUTT-3' and antisense: 5'-ACGUGACAC GUUCGGAGAATT-3'), or 100 nM miR-196a-5p inhibitor (5'-CCCAACAACAUGAAACUACCUA-3') or inhibitor NC (5'-CAGUACUUUUGUGUAGU ACAA-3') were transfected into E2-treated RL95-2 and ECC-1 cells using Lipofectamine 2000 (Invitrogen, USA) according to the manufacturer's protocol at 37˚C for 6h. To inhibit FOXO1, 0.2 μM of FOXO1 si-RNA (sense: 5'-CUGCAUAGCAUCAAGUCUU-3' and antisense: 5'-AAGACUUGAUGCUAUGCAG-3') or 0.2 μM of negative control siRNA (si-NC; 5'-TTCTCCGAACGTGTCACGT-3') were transfected using Lipofectamine 2000 at 37°C for 6h. After transfection for 48h, cells were harvested and transfection efficiency was determined by quantitative (q)PCR.

Cell viability assessment

Cells (5×10^4 cells/well) were seeded into 96-well plates (Corning) and incubated at 37°C for 24h until the cells reached 70% confluency. Next, 100 mL of 3-(4,5-dimethylthiazol-2-yl)-2,5-diphenyltetrazolium bromide (MTT) reagent (0.5 mg/ml, Sigma-Aldrich) was added for 4h at 37°C, followed by the addition of 150 μL DMSO. The absorbance was measured at 570 nm with a microplate reader.

Transcription-quantitative PCR (RT-qPCR)

The mirVana miRNA isolation kit (Ambion, USA) was employed to isolate total RNA as recommended by the manufacturer. cDNA was synthesized with a cDNA synthesis kit (Beyotime, China). Next, the PCR analysis was carried out by the TaqMan miRNA-specific assay (Applied Biosystems, USA) following the manufacturer's protocol. The PCR program was 95°C for 10 min, followed by 40 cycles of 95°C for 10 s, 60°C for 20 s and 72°C for 30 s on a 7000 Real-Time system (Applied Biosystems). The relative miR-196a-5p level was normalized against U6 RNA using the $2^{-\Delta\Delta Ct}$ method (Livak and Schmittgen 2001). GAPDH served as a control. The primers for amplification are detailed in Table 1.

Wound healing assay

Transfected cells (5×10^5 cells/well) were incubated in 12-well plates (Corning) at 37°C for 24h. When cells

Table 1. Primer pairs for amplification.

Gene	Sequences (5'-3')	
miR-196a-5p	Sense	CCGACGTAGGTAGTTTCATGTT
	Anti-sense	GTGCAGGGTCCGAGGTATTC
GAPDH	Sense	CGGCTACCACATCCAAGGAA
	Anti-sense	AGCCACATCGCTCAGACACC
U6	Sense	CTCGCTTCGGCAGCACA
	Anti-sense	AACGCTTCACGAATTTGCGT

reached 80% confluency, a 1-mm pipette tip was used to scrape the cell layer in a straight line. After gently removing the detached cells, attached cells were incubated in fresh serum-free RPMI-1640 medium for another 24h, and subsequently images were taken at 100× magnification using a phase contrast microscope (Leitz Ortholux II, Germany). The width of the wound was determined using ImageJ (version 1.52, NIH, USA).

Transwell assay

For cell migration assays, 100 µL of transfected cells (1×10^5 cells) were suspended in RPMI-1640 medium and placed in the upper chamber of Transwells (8-µm pore size, Corning) for 24h at 37°C. In the basolateral chamber, medium with 20% FBS was added as a chemo-attractant. Cells which migrated through the membrane were immersed in 70% ethanol for 10 min and then stained with 0.2% Crystal Violet for 10 min at 25°C. An Olympus IX70 inverted microscope (Japan) was used to visualize stained cells in five randomly selected visual fields, which were counted by ImageJ software.

For cell invasion determination, 50 µL of Matrigel (BD Biosciences, USA) was added and incubated for 30 min at 37°C to form a thin gel layer in the upper chambers of transwells. The same procedures were then performed as described for the Transwell migration assay.

Luciferase reporter assays

Targetscan (release 7.2, http://www.targetscan.org/) was used to obtain the target genes and binding sites of miR-196a-5p. The pmirGLO plasmid (LMAI Bio, China) was employed to clone 3'-UTRs from FOXO1 containing wild-type (wt) and mutant (mut) miR-196a-5p binding sequences. Subsequently, cells were co-transfected with wt/mut FOXO1 and miR-196a-5p mimic for 6h at 37°C using Lipofectamine 2000. After incubation for 48h, the dual-luciferase reporter assay system (Promega, USA) was utilized for luciferase activity assessments, which were normalized to Renilla luciferase activity.

Flow cytometry

Cell apoptosis was measured as previously reported (Zembruski et al., 2012). Cells (5×10^4 cells/well) were incubated in 6-well plates for 48h at 37°C. Next, cells were stained with 5 µL of 7-AAD and 5 µl Annexin V-PE for 20 min on ice in the dark. After centrifugation at 400×g for 5 min at 4°C, samples were resuspended in cold PBS. Cell apoptosis was analyzed by a CytoFlex cytometer (Beckman Coulter, USA) within 1h and quantified by FlowJo software (Version 7.5, Tree Star, USA).

Western blot analysis

RIPA buffer (Bioteke, China) was used to extract proteins. Next, proteins were resolved by 12% SDS-PAGE and transferred to polyvinylidene difluoride membranes, which were then blocked with 5% non-fat milk for 1h at 25°C. The membranes were incubated with primary monoclonal antibodies against FOXO1 (Cat. no. sc-374427; 1:100, Santa Cruz, USA), Bcl-2 (Cat. no. sc-7382; 1:200, Santa Cruz), Bax (Cat. no. sc-7480; 1:200, Santa Cruz), Caspase 3 (Cat. no. ab32351; 1:5,000, Abcam, USA), and β-actin (Cat. no. sc-47778; 1:200, Santa Cruz) overnight at 4°C. The membranes were then incubated with secondary antibody conjugated to horseradish peroxidase (Cat. no. sc-2005 1:2,000; Santa Cruz) for 2h at 25°C and visualized with an ECL detection system (Amersham, USA) following the manufacturer's protocol. β-actin served as an internal control. Quantification was conducted using ImageJ software.

Statistical analysis

Results were analyzed by SPSS software (Version 17.0, SPSS Inc., USA) and data were expressed as means ± SD. One-way ANOVA with Tukey's post hoc tests were utilized to assess differences among multiple groups. $P<0.05$ was considered statistically significant.

Results

E2 promotes cell viability and miR-196a-5p expression in RL95-2, HEC-1B and ECC-1 cells

Different concentrations of E2 (2.5, 5, 10 and 20 nM) were administered to RL95-2, HEC-1B and ECC-1 cells and cell viability was subsequently determined. Fig. 1A,C,D show that E2 induced a significant increase in cell viability compared to untreated RL95-2, HEC-1B and ECC-1 cells ($P<0.05$). In addition, E2-treated miR-196a-5p was significantly up-regulated in both ECC-1 and RL95-2 cells ($P<0.05$). However, in HEC-1B cells, there was no difference in the expression of E2-treated miR-196a-5p in 2.5 and 5 nM, (Fig. 1B,D,E). In summary, these results indicate that E2 promotes cell viability and increases the expression of miR-196a-5p in RL95-2 and ECC-1 cells, so RL95-2 and ECC-1 cells were selected for subsequent experiments.

The miR-196a-5p induced cell growth in E2-treated RL95-2 and ECC-1 cells

Next, miR-196a-5p mimic or inhibitor was transfected into E2-treated RL95-2 and ECC-1 cells. Fig. 2A,F show that miR-196a-5p expression was enhanced after E2 treatment when compared with the control group ($P<0.05$); meanwhile, miR-196a-5p mimic significantly induced miR-196a-5p expression in E2-treated RL95-2 and ECC-1 cells ($P<0.05$). However, miR-196a-5p inhibitor produced a remarkable reduction in miR-196a-5p expression ($P<0.05$). Similar results were found for cell viability (Fig. 2B,G). Inhibition of

miR-196a-5p visibly reversed the increase in cell viability induced by miR-196a-5p in E2-treated RL95-2 and ECC-1 cells. As displayed in Fig. 2C-D,H-I, E2 treatment suppressed RL95-2 and ECC-1 cell apoptosis, and miR-196a-5p mimic further inhibited cell apoptosis compared with the mimic NC group (mimic group decreased slightly, but $P>0.05$), but inhibition of miR-196a-5p blocked this process ($P<0.05$). Western blot analysis showed that E2-treated RL95-2 and ECC-1 cells exhibited increased Bcl-2 expression but reduced Bax and Caspase 3 expression following miR-196a-5p mimic transfection ($P<0.05$), while miR-196a-5p inhibitor significantly downregulated Bcl-2 expression but upregulated Bax and Caspase 3 compared with inhibitor NC ($P<0.05$) (Fig. 2E,J).

miR-196a-5p promoted migration and invasion of E2-treated RL95-2 and ECC-1 cells

A scratch wound was produced in monolayers of RL95-2 and ECC-1 cells and evaluated 24h later. E2 treatment resulted in decreased wound width which was further reduced by miR-196a-5p treatment. In contrast, miR-196a-5p inhibitor dramatically expanded wound width compared with inhibitor NC. Transwell assay was used to detect the invasion of RL95-2 and ECC-1 cells. Compared with the control group, the results showed that overexpression of miR-196a-5p significantly promoted E2-induced invasion of RL95-2 and ECC-1 cells, and knocking down miR-196a-5p reversed the above effects. Fig. 3A-F show that miR-196a-5p

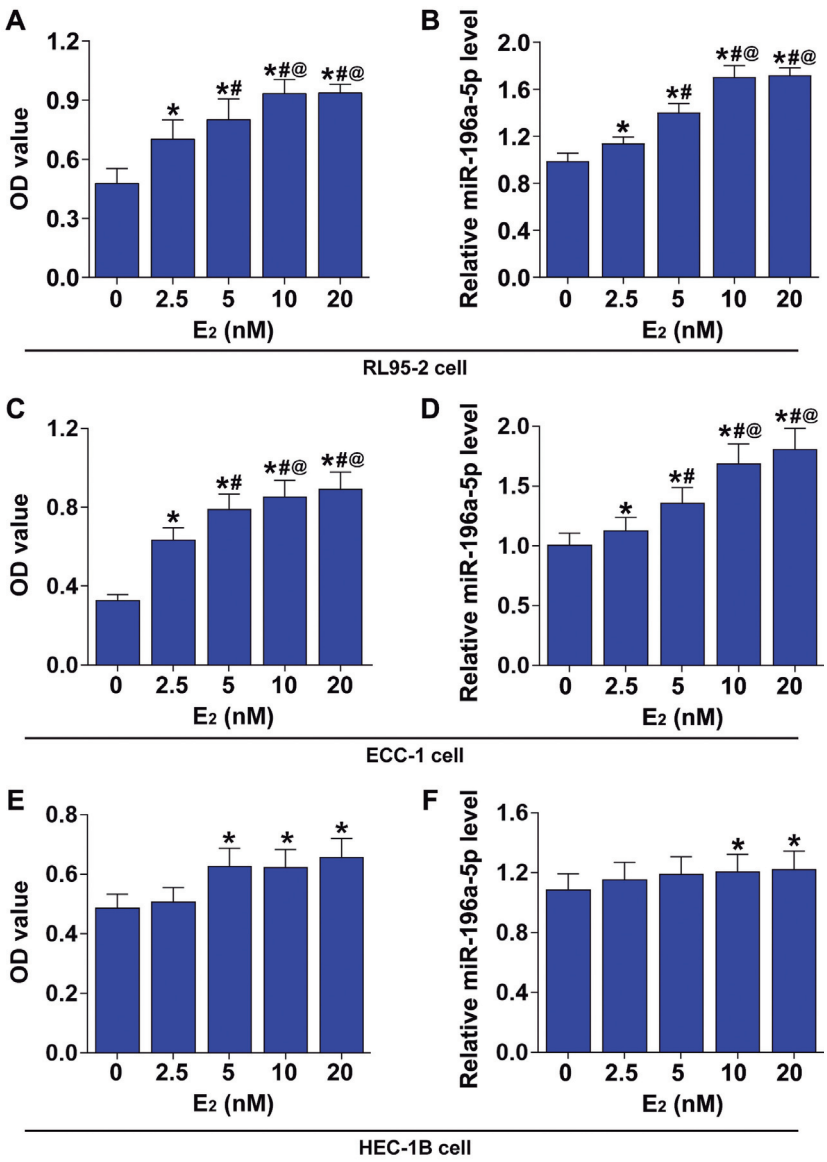

Fig. 1. E2 promoted cell viability and increased miR-196a-5p expression in RL95-2, HEC-1B and ECC-1 cells. **A, C, E.** Cell viability was evaluated using MTT assay. **B, D, F.** The relative miR-196a-5p level was measured using RT-PCR. *P<0.05 versus untreated RL95-2, HEC-1B and ECC-1 cells. There were 40 cases of "N" in each experimental group.

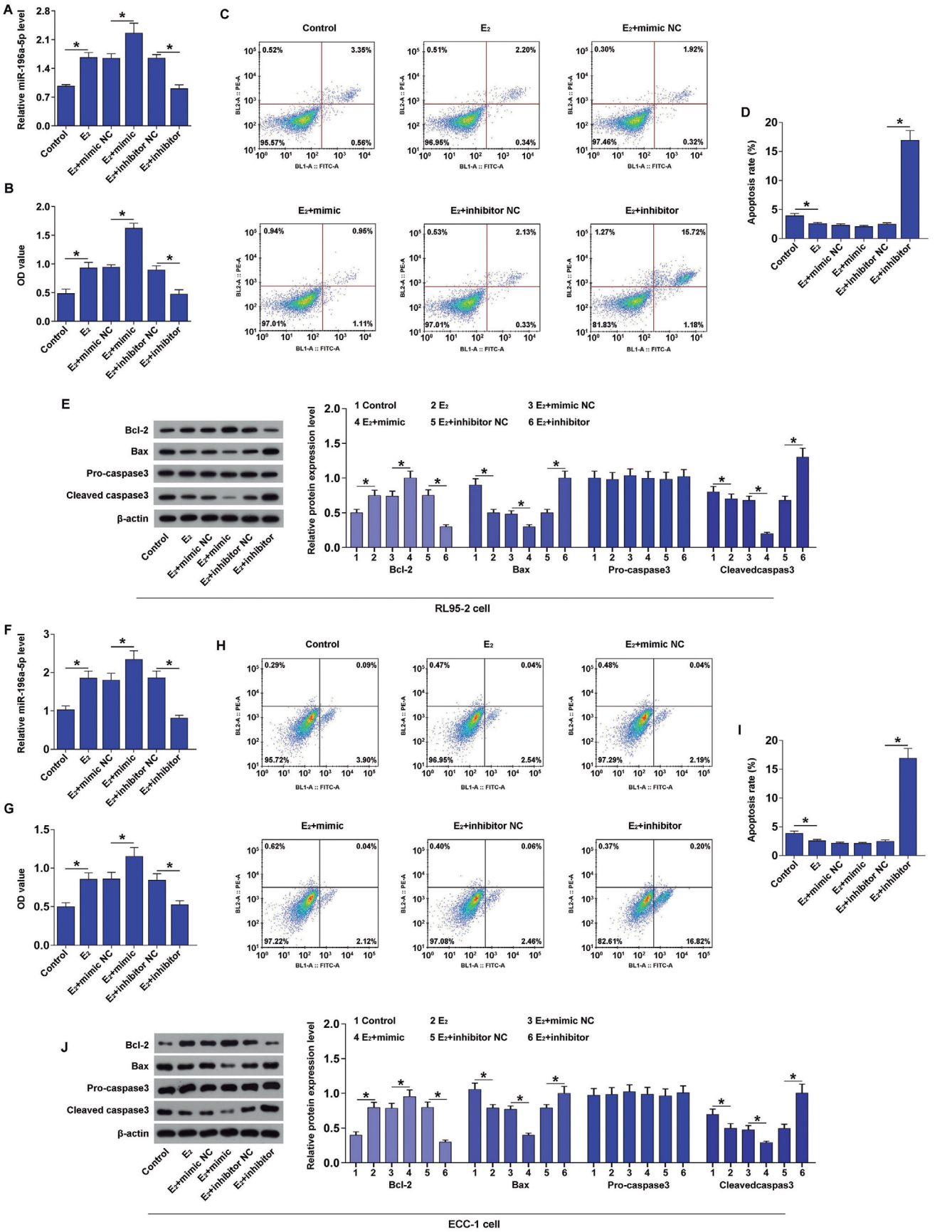

Fig. 2. miR-196a-5p induced cell growth in E2-treated RL95-2 and ECC-1 cells. **A, F.** The relative miR-196a-5p level was determined following miR-196a-5p mimic/inhibitor transfection. **B, G.** Cell viability was assessed following miR-196a-5p mimic/inhibitor transfection. **C, D, H, I.** Apoptotic cells were assessed by flow cytometry following miR-196a-5p mimic/inhibitor transfection. **E, J.** Bcl-2, Bax and Caspase 3 levels were quantified by immunoblotting. *P<0.05.

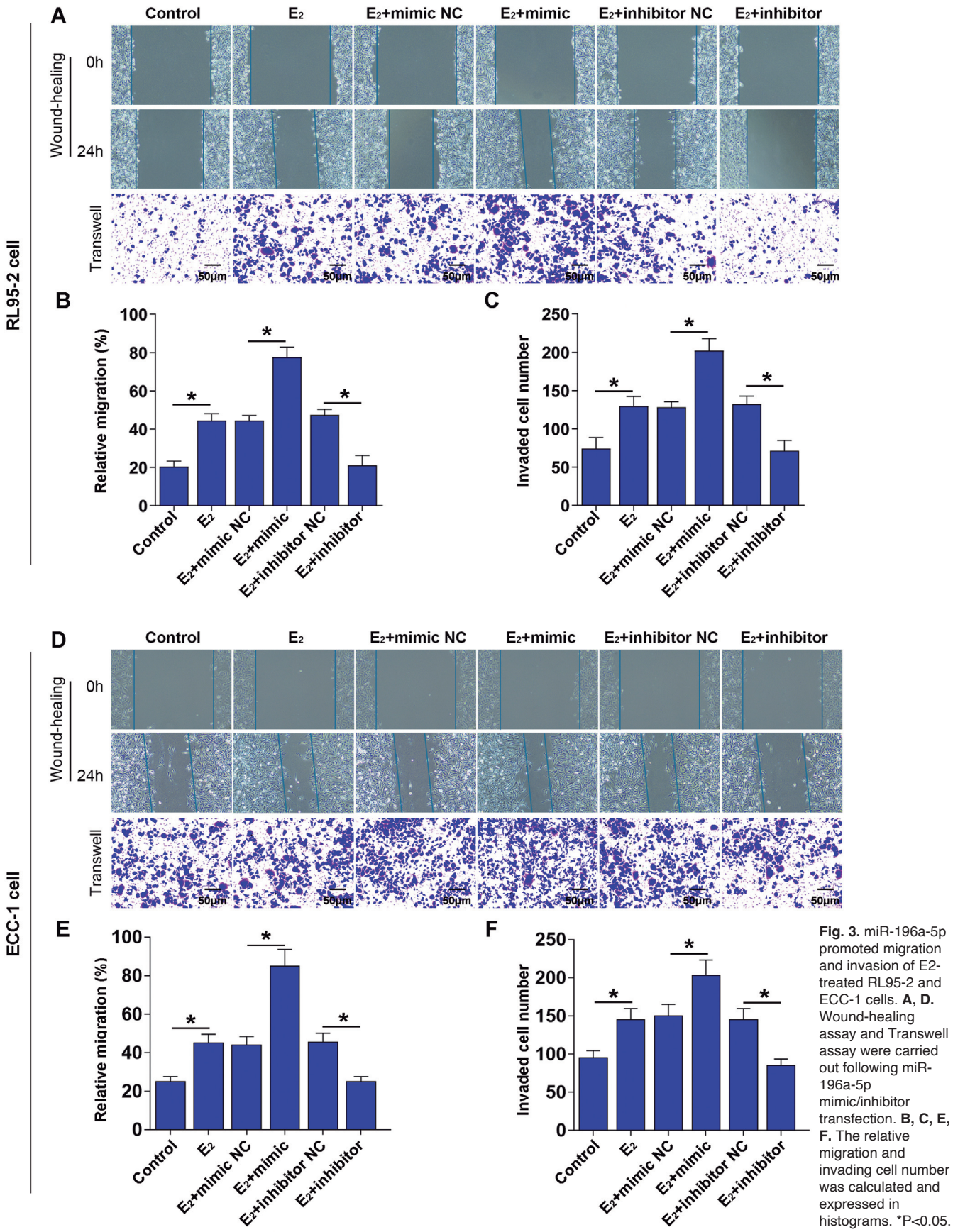

Fig. 3. miR-196a-5p promoted migration and invasion of E2-treated RL95-2 and ECC-1 cells. **A, D.** Wound-healing assay and Transwell assay were carried out following miR-196a-5p mimic/inhibitor transfection. **B, C, E, F.** The relative migration and invading cell number was calculated and expressed in histograms. *P<0.05.

distinctly facilitated cell migration and invasion by E2-treated RL95-2 and ECC-1 cells, while suppression of miR-196a-5p blocked this process.

miR-196a-5p targets FOXO1

Bioinformatics analysis was used to identify a binding site for miR-196a-5p in the 3′-UTR of FOXO1. Luciferase reporter constructs were then created containing wt miR-196a-5p binding sequence (ACUACCU) and mut sequence (UGAUGGA) (Fig. 4A). A luciferase assay was performed in cells transfected with a miR-196a-5p mimic or inhibitor and it was found that transfection with miR-196a-5p and wt FOXO1 luciferase constructs resulted in a significant decrease in luciferase activity as compared with the mimic NC group ($P<0.05$), while luciferase activity from the construct containing mut FOXO1 3′-UTR sequence was not affected (Fig. 4B,E). Subsequently, the results of qRT-PCR and Western blot showed that E2 decreased the expression of FOXO1 protein in RL95-2 and ECC-1 cells, and compared with the control group (mimic-NC

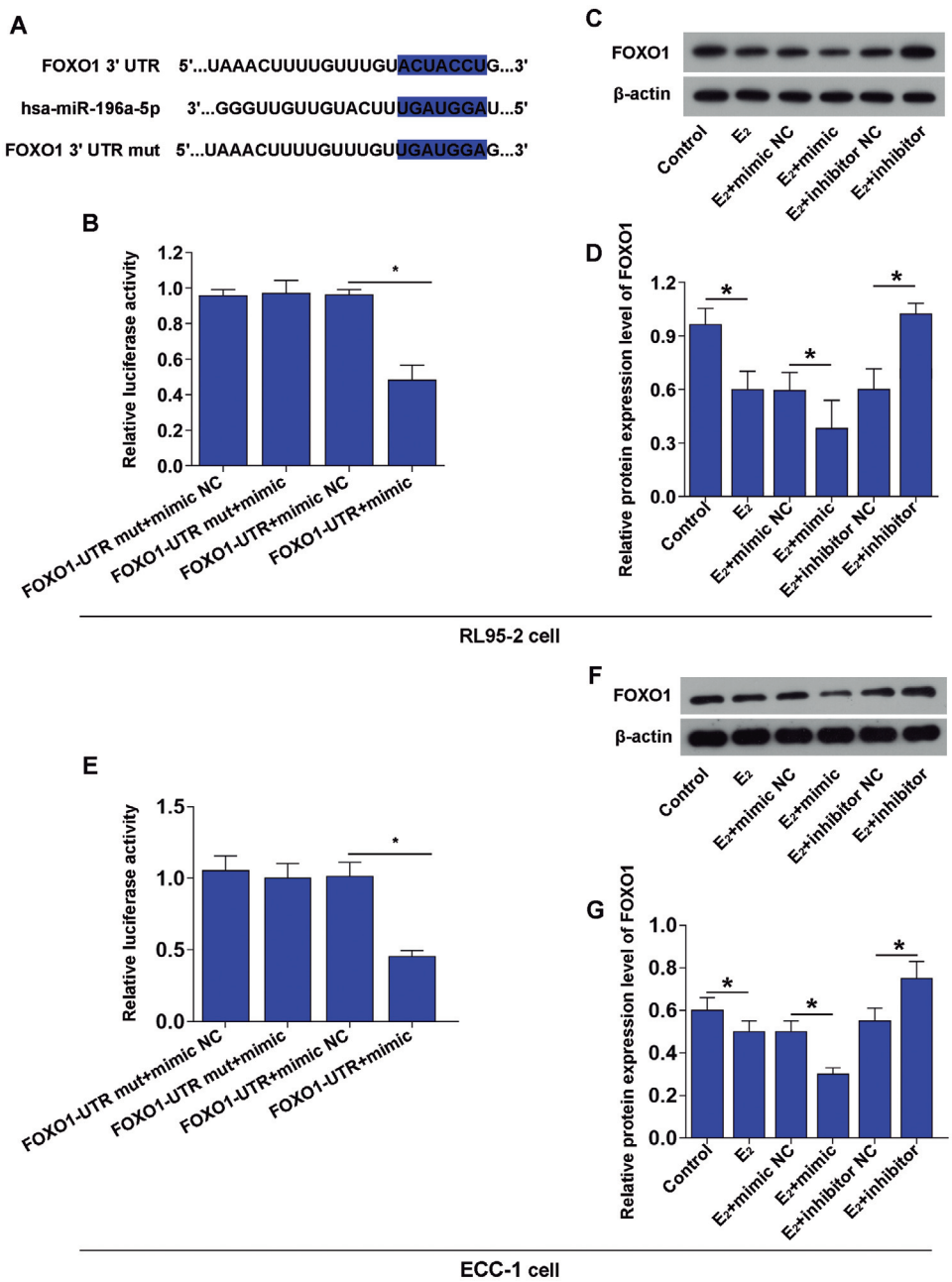

Fig. 4. miR-196a-5p targets FOXO1. **A.** The binding site was determined using Targetscan. **B, E.** Luciferase activity was assessed after co-transfection with FOXO1-wt/mut and miR-196a-5p. **C, D, F, G.** FOXO1 was quantified after miR-196a-5p mimic/inhibitor transfection. *P<0.05.

or inhibitor NC), overexpression of miR- 212-5p significantly inhibited the expression of FOXO1 mRNA and protein (P<0.05). MiR-212-5p inhibitor significantly promoted the expression of FOXO1 mRNA and protein (P<0.05) Fig. 4C,D,F,G.

Transfection with si-FOXO1 alleviates the effects of miR-196a-5p inhibitor on cell growth of E2-treated RL95-2 and ECC-1

FOXO1 siRNA was transfected into E2-treated RL95-2 and ECC-1 cells. Figure 5A,B,H,I show that si-FOXO1 induced a significant decrease in FOXO1 expression vs si-NC (P<0.05). Figure C,J indicate that the cell proliferation rate of si-FOXO1 group was higher than that of NC group (P<0.05). Meanwhile, si-FOXO1+miR-196a-5p inhibitors inhibit cell viability. Fig. 5D-E,K-L show that si-FOXO1 resulted in a lower apoptosis rate than in the NC group (P<0.05); meanwhile, si-FOXO1 + miR-196a-5p inhibitor induced cell apoptosis. Western blot analysis revealed that si-FOXO1 significantly elevated Bcl-2 expression but repressed Bax and Caspase 3 expression (P<0.05), while si-FOXO1 and miR-196a-5p inhibitor downregulated Bcl-2 expression but upregulated expression of Bax and Caspase 3 (P<0.05; Fig. 5F-G,M-N).

si-FOXO1 inhibits the effects of miR-196a-5p inhibitor on the migration and invasion of E2-treated RL95-2 and ECC-1 cells

As depicted in Fig. 6A-F, inhibition of miR-196a-5p resulted in a larger wound width. Transfection with si-FOXO1 dramatically decreased the wound width, while si-FOXO1 + miR-196a-5p inhibitor reversed the effect of si-FOXO1 on wound-healing. Transwell assays revealed that miR-196a-5p inhibitor visibly repressed the migration and invading numbers of E2-treated RL95-2

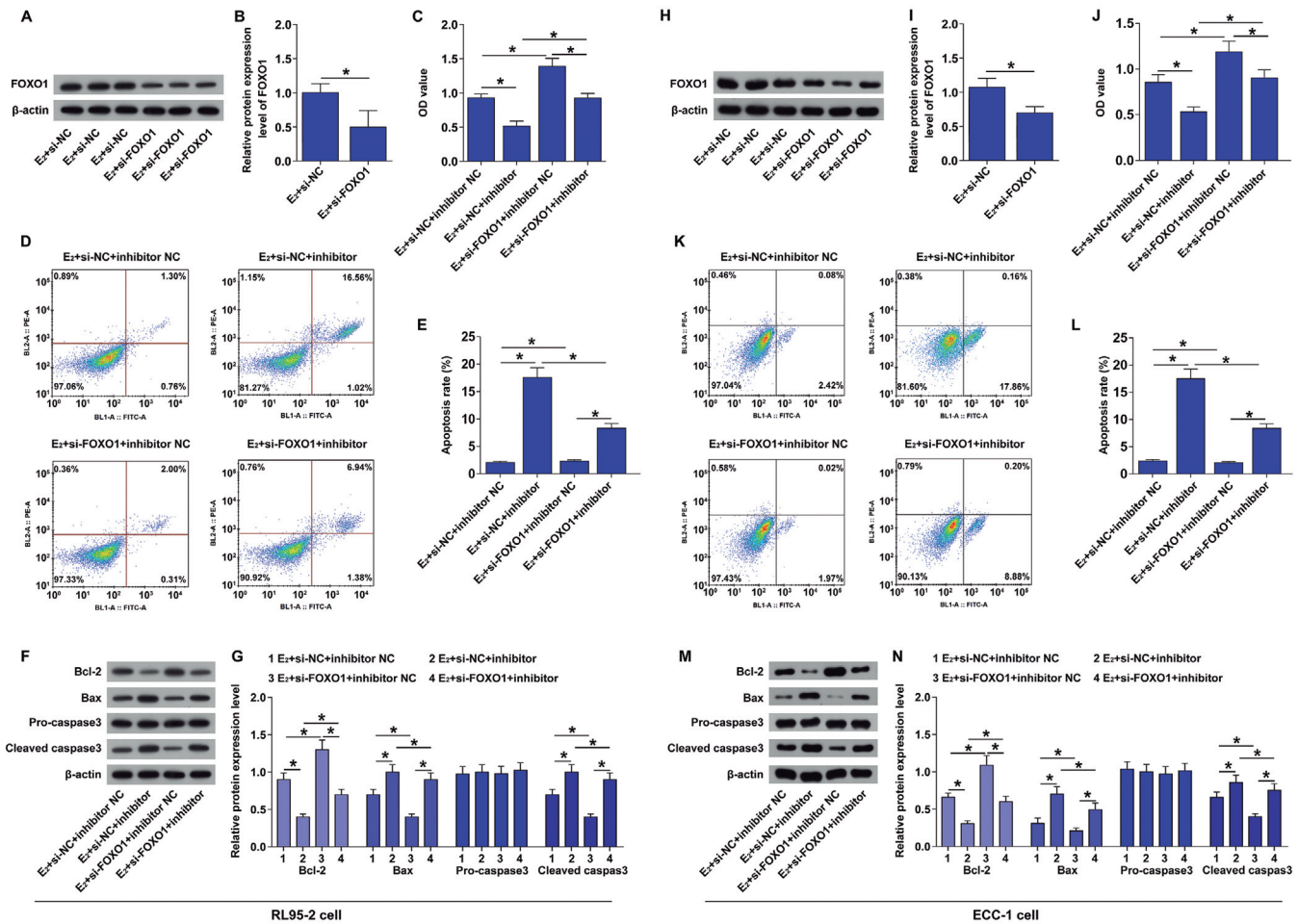

Fig. 5. Transfection with si-FOXO1 alleviates the effects of miR-196a-5p inhibitor on cell growth of E2-treated RL95-2 and ECC-1 cells. **A, B, H, I.** Protein level of FOXO1 was determined following si-FOXO1 transfection. **C, J.** Cell viability was measured following si-FOXO1 and/or miR-196a-5p inhibitor transfection. **D, E, K, L.** Cell apoptosis was assessed following si-FOXO1 and/or miR-196a-5p inhibitor transfection. **F, G, M, N.** Bcl-2, Bax and Caspase 3 expression was determined following si-FOXO1 and/or miR-196a-5p inhibitor transfection. *P<0.05.

and ECC-1 cells when compared with the NC group ($P<0.05$), while transfection with si-FOXO1 significantly promoted the migration and invasion of E2-treated RL95-2 and ECC-1 cells ($P<0.05$). In contrast, transfection with si-FOXO1 together with miR-196a-5p inhibitor suppressed cell migration and invasion ($P<0.05$) (Fig. 6A-F).

Discussion

Estrogens are the most important steroid hormone produced by the ovaries and placenta (Zeng et al., 2018). Estrogens regulate many functions, for example, female reproductive system, bone excretory system, in the human organism (Vivacqua et al., 2018). Estrogens play a major role in physiological changes or pathological changes, Estradiol (E2) is the main component of estrogen (Kim, 2021). Most studies have shown that E2 is involved in endometrial cancer progression, such as E2 induced UBE2C expression via estrogen receptor α, which binds directly to the UBE2C promoter element. Silencing of UBE2C inhibited E2-promoted migration, invasion, and EMT *in vitro* and *in vivo* (Liu et al., 2020). BKCa participates in E2 inducing endometrial adenocarcinoma by activating the MEK/ERK pathway (Wang et al., 2018). More importantly, 17β- estradiol protects ATDC5 chondrocytes from mitochondrial autophagy by stimulating the expression of GPER/GPR30 (Fan et al., 2018). In this study, we found that E2 significantly enhanced the cell viability of RL95-2 and ECC-1 cells in a dose-dependent manner. Further studies showed that E2 treatment significantly increased RL95-2 and ECC-1 cells proliferative activity, migration and invasion, and inhibited apoptosis.

MiRNAs are a category of non-coding microRNAs of 22-24nt, which are numerous and functionally complex, and modulate target protein expression after transcription via combining with the 3' untranslated region of target mRNAs (Mao et al., 2020; Chen et al., 2021). miRNAs can act as tumor promoters or inhibitors to regulate cell multiplication, differentiation and apoptosis, and are widely involved in the regulation of many life processes (Cao et al., 2020). There is increasing evidence that miRNAs are novel biomarkers (He et al., 2021). Here we focused on miR-196a. A study revealed aberrant serum levels of miR-196a and miR-196b in patients with high tumor grade and metastatic osteosarcoma, and suggested that miR-196a and miR-196b may be underlying biomarkers of prognostic significance (Zhang et al., 2014). Liu and colleagues demonstrated that miRNA-196a

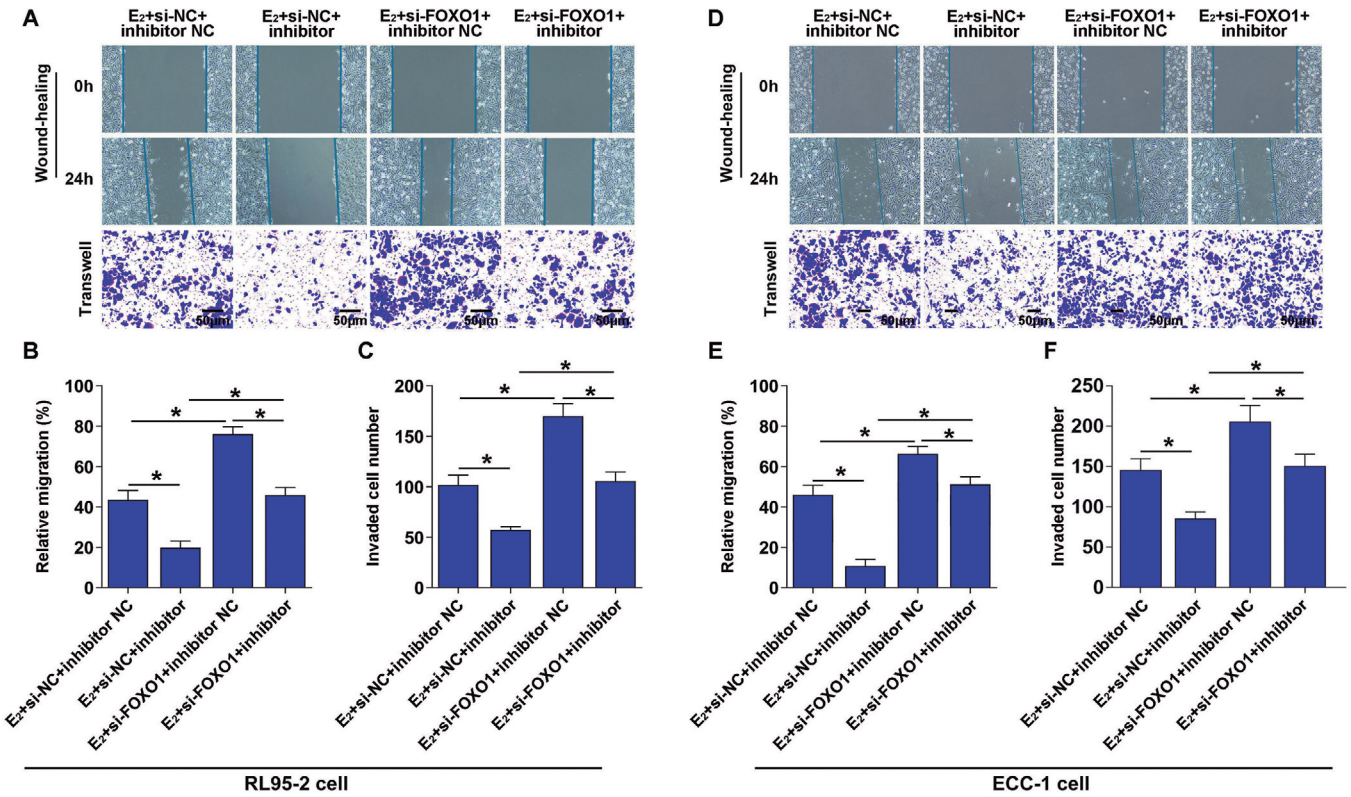

Fig. 6. si-FOXO1 inhibits the effects of miR-196a-5p inhibitor on the migration and invasion of E2-treated RL95-2 and ECC-1 cells. **A, D.** Wound-healing assay and Transwell assays were conducted following si-FOXO1 and/or miR-196a-5p inhibitor transfection. **B, C, E, F.** The relative migration and invading cell number was calculated and expressed in histograms. *P<0.05.

expression was excessive in lung cancer tissues and cells, while inhibition of miRNA-196a reduced cell viability, growth, self-renewal and stemness by activating glutathione peroxidase 3 (Liu et al., 2019). Another study also demonstrated that the level of miR-196b enhanced hepatocellular carcinoma (HCC) cell migration and invasion, which was inhibited by antagonizing miR-196b (Yu et al., 2018). In addition, miR-196a was upregulated in cervical cancer, but inhibiting miR-196a repressed cell proliferation and cell cycle transition (Hou et al., 2014). Consistent with the aforementioned results, we found that miR-196a-5p expression was upregulated in E2-treated RL95-2 and ECC-1 cells and that the miR-196a-5p mimic promotes E2-induced cell viability, migration and invasion, and inhibited apoptosis. The miR-196a-5p inhibitor blocked this process, supporting the conclusion that inhibition of miR-196a-5p may attenuate estrogen-dependent endometrial cancer.

Forkhead box protein O1 (FOXO1), belonging to O subclass of FOX, mainly functions as a transcription factor which participates in diverse signaling pathways and biological processes, including lipid metabolism, apoptosis and oxidative stress reactions (Sparks and Dong, 2009; Prasad et al., 2014; Liang et al., 2021). FOXO1 functions as a target of diverse miRNAs in cancers. He et al. found that FOXO1 served as a target of miR-374a in osteosarcoma and that inhibiting FOXO1 was essential for osteosarcoma cell proliferation (He et al., 2015). Previous studies have demonstrated that repression of FOXO1 provoked cell proliferation but suppressed apoptosis in papillary thyroid carcinoma cells (Song et al., 2015) and lung cancer (Zhao et al., 2014). In HCC cells, miR-135a expression was elevated and miR135a promoted cell migration and invasion by directly targeting FOXO1 (Zeng et al., 2016). Yang and his colleagues demonstrated that FOXO1 3'-UTR bound to miR-9 and served as an inhibitor of miR-9 in breast cancer cell metastasis (Yang et al., 2014). Furthermore, a recent study indicated that FOXO1 was negatively regulated by miR-205-5p, which resulted in paclitaxel resistance and endometrial cancer proliferation (Lu et al., 2019). Another study also revealed that miR-9, -27, -96, -153, -182, -183, or -186 decreased the level of FOXO1, but inhibition of these miRNAs reversed the decrease in FOXO1, G1 arrest and cell death, which was inhibited by transfection of si-FOXO1 in endometrial cancer cells (Myatt et al., 2010). In this study, we found that FOXO1 is the target gene of miR-196a-5p, and miR-212-5p directly targets FOXO1 to promote proliferation, migration and invasion of E2-induced endometrial cancer cells and inhibit apoptosis.

Although the role of miR-196a-5p in estrogen-dependent endometrial cancer *in vitro* has been confirmed, further *in vitro* experiments and clinical practice are still needed. In addition to miR-196a-5p and its target gene FOXO1, other potential diagnostic and therapeutic miRNA signatures should be explored to improve the diagnosis and treatments for estrogen-dependent endometrial cancer.

In summary, we found and confirmed that miR-196a-5p is upregulated in E2-induced endometrial cancer cells, miR-196a-5p targets FOXO1 promoting the proliferation, migration and invasion of E2-induced endometrial cancer cells, and inhibiting cell apoptosis; Knocking down miR-196a-5p will reverse this process. Our study further elucidates the molecular mechanism of estrogen-dependent endometrial carcinogenesis and progression, and proposes that miR-196a-5p may serve as a possible therapeutic target for estrogen-dependent endometrial cancer.

Acknowledgements. Not applicable.

Funding. This work was financially supported by the Sci-Tech Planning Project of Jiaxing (Number: 2020AD30115 to ZYZ).

Conflicts of interest. The Authors declare that there is no conflict of interest.

References

Banno K., Iida M., Yanokura M., Kisu I., Iwata T., Tominaga E., Tanaka K. and Aoki D. (2014). MicroRNA in cervical cancer: OncomiRs and tumor suppressor miRs in diagnosis and treatment. ScientificWorldJournal. 2014, 178075.

Bokhman J.V. (1983). Two pathogenetic types of endometrial carcinoma. Gynecol. Oncol. 15, 10-17.

Cao, Z., Qiu J., Yang G., Liu Y., Luo W., You L., Zheng L. and Zhang T. (2020). MiR-135a biogenesis and regulation in malignancy: a new hope for cancer research and therapy. Cancer Biol. Med. 17, 569-582.

Chen C.G., Luo B.S. and Wang C. (2021). Potential role of miR-425, miR-155 and miR-33 in Streptococcus pneumoniae pneumonia by using bioinformatics analysis and experimental validation. J. Biol. Regul. Homeost. Agents 35, 953-964.

Chen J., Gao F. and Liu N. (2018). L1CAM promotes epithelial to mesenchymal transition and formation of cancer initiating cells in human endometrial cancer. Exp. Ther. Med. 15, 2792-2797.

Doll A., Abal M., Rigau M., Monge M., Gonzalez M., Demajo S., Colás E., Llauradó M., Alazzouzi H., Planagumá J., Lohmann M.A., Garcia J., Castellvi S., Ramon y Cajal J., Gil-Moreno A., Xercavins J., Alameda F. and Reventós J. (2008). Novel molecular profiles of endometrial cancer-new light through old windows. J. Steroid Biochem. Mol. Biol. 108, 221-229.

Fan D.X., Yang X.H., Li Y.N. and Guo L. (2018). 17β-estradiol on the expression of G-protein coupled estrogen receptor (GPER/GPR30) mitophagy, and the PI3K/Akt signaling pathway in ATDC5 chondrocytes *in vitro*. Med. Sci. Monit. 24, 1936-1947.

He W., Feng L., Xia D. and Han N. (2015). MiR-374a promotes the proliferation of human osteosarcoma by downregulating FOXO1 expression. Int. J. Clin. Exp. Med. 8, 3482-3489.

He Y., Jiang X., Duan L., Xiong Q., Yuan Y., Liu P., Jiang L., Shen Q., Zhao S., Yang C. and Y. Chen Y. (2021). LncRNA PKMYT1AR promotes cancer stem cell maintenance in non-small cell lung cancer via activating Wnt signaling pathway. Mol. Cancer 20, 156.

Hirata H., Ueno K., Shahryari V., Tanaka Y., Tabatabai Z.L., Hinoda Y. and Dahiya R. (2012). Oncogenic miRNA-182-5p targets Smad4 and RECK in human bladder cancer. PLoS One 7, e51056.

Hou T., Ou J., Zhao X., Huang X., Huang Y. and Zhang Y. (2014).

MicroRNA-196a promotes cervical cancer proliferation through the regulation of FOXO1 and p27Kip1. Br. J. Cancer 110, 1260-1268.

Kim I.S. (2021). Current perspectives on the beneficial effects of soybean isoflavones and their metabolites for humans. Antioxidants (Basel) 10, 1064.

Kong D., Piao Y.S., Yamashita S., Oshima H., Oguma K., Fushida S., Fujimura T., Minamoto T., Seno H., Yamada Y., Satou K., Ushijima T., Ishikawa T.O. and Oshima M. (2012). Inflammation-induced repression of tumor suppressor miR-7 in gastric tumor cells. Oncogene 31, 3949-3960.

Lee Y.M., Lee J.Y., Ho C.C., Hong Q.S., Yu S.L., Tzeng C.R., Yang P.C. and Chen H.W. (2011). miRNA-34b as a tumor suppressor in estrogen-dependent growth of breast cancer cells. Breast Cancer Res. 13, R116.

Liang X., Su Y. and Huo Y. (2021). Forkhead box protein O1 (FoxO1) /SERPINB1 ameliorates ROS production in diabetic nephropathy. Food Sci. Nutr. 9, 44-51.

Liu Q., Bai W., Huang F., Tang J. and Lin X. (2019). Downregulation of microRNA-196a inhibits stem cell self-renewal ability and stemness in non-small-cell lung cancer through upregulating GPX3 expression. Int. J. Biochem. Cell Biol. 115, 105571.

Liu X., Sempere L.F., Ouyang H., Memoli V.A., Andrew A.S., Luo Y., Demidenko E., Korc M., Shi W., Preis M., Dragnev K.H., Li H., Direnzo J., Bak M., Freemantle S.J., Kauppinen S. and Dmitrovsky E. (2010). MicroRNA-31 functions as an oncogenic microRNA in mouse and human lung cancer cells by repressing specific tumor suppressors. J. Clin. Invest. 120, 1298-1309.

Liu Y., Zhao R., Chi S., Zhang W., Xiao C., Zhou X., Zhao Y. and Wang H. (2020). UBE2C is upregulated by estrogen and promotes epithelial-mesenchymal transition via p53 in endometrial cancer. Mol. Cancer Res. 18, 204-215.

Livak K.J. and Schmittgen T.D. (2001). Analysis of relative gene expression data using real-time quantitative PCR and the 2(-Delta Delta C(T)) Method. Methods 25, 402-408.

Lu Z., Xu Y., Yao Y. and Jiang S. (2019). miR-205-5p contributes to paclitaxel resistance and progression of endometrial cancer by downregulating FOXO1. Oncol. Res. (in press).

Mao Q.Q., Chen J.J., Xu W.J., Zhao X.Z., Sun X. and Zhong L. (2020). miR-92a-3p promotes the proliferation and invasion of gastric cancer cells by targeting KLF2. J. Biol. Regul. Homeost. Agents 34, 1333-1341.

Morice P., Leary A., Creutzberg C., Abu-Rustum N. and Darai E. (2016). Endometrial cancer. Lancet 387, 1094-1108.

Myatt S.S., Wang J., Monteiro L.J., Christian M., Ho K.K., Fusi L., Dina R.E., Brosens J.J., Ghaem-Maghami S. and Lam E.W. (2010). Definition of microRNAs that repress expression of the tumor suppressor gene FOXO1 in endometrial cancer. Cancer Res. 70, 367-377.

Pan Y., Shu X., Sun L., Yu L., Sun L., Yang Z. and Ran Y. (2017). miR-196a-5p modulates gastric cancer stem cell characteristics by targeting Smad4. Int. J. Oncol. 50, 1965-1976.

Prasad S.B., Yadav S.S., Das M., Govardhan H.B., Pandey L.K., Singh S., Pradhan S. and Narayan G. (2014). Down regulation of FOXO1 promotes cell proliferation in cervical cancer. J. Cancer 5, 655-662.

Pu M., Chen J., Tao Z., Miao L., Qi X., Wang Y. and Ren J. (2019). Regulatory network of miRNA on its target: coordination between transcriptional and post-transcriptional regulation of gene expression. Cell Mol. Life Sci. 76, 441-451.

Setiawan V.W., Yang H.P., Pike M.C., McCann S.E., Yu H., Xiang Y.B., Wolk A., Wentzensen N., Weiss N.S., Webb P.M., van den Brandt P.A., van de Vijver K., Thompson P.J., Strom B.L., Spurdle A.B., Soslow R.A., Shu X.O., Schairer C., Sacerdote C., Rohan T.E., Robien K., Risch H.A., Ricceri F., Rebbeck T.R., Rastogi R., Prescott J., Polidoro S., Park Y., Olson S.H., Moysich K.B., Miller A.B., McCullough M.L., Matsuno R.K., Magliocco A.M., Lurie G., Lu L., Lissowska J., Liang X., Lacey J.V. Jr., Kolonel L.N., Henderson B.E., Hankinson S.E., Håkansson N., Goodman M.T., Gaudet M.M., Garcia-Closas M., Friedenreich C.M., Freudenheim J.L., Doherty J., De Vivo I., Courneya K.S., Cook L.S., Chen C., Cerhan J.R., Cai H., Brinton L.A., Bernstein L., Anderson K.E., Anton-Culver H., Schouten L.J. and Horn-Ross P.L. (2013). Type I and II endometrial cancers: have they different risk factors? J. Clin. Oncol. 31, 2607-2618.

Song H.M., Song J.L., Li D.F., Hua K.Y., Zhao B.K. and Fang L. (2015). Inhibition of FOXO1 by small interfering RNA enhances proliferation and inhibits apoptosis of papillary thyroid carcinoma cells via Akt/FOXO1/Bim pathway. Onco Targets Ther. 8, 3565-3573.

Sparks J.D. and Dong H.H. (2009). FoxO1 and hepatic lipid metabolism. Curr. Opin. Lipidol. 20, 217-226.

Vivacqua A., Sebastiani A., Miglietta A.M., Rigiracciolo D.C., Cirillo F., Galli G.R., Talia M., Santolla M.F., Lappano R., Giordano F., Panno M.L. and Maggiolini M. (2018). miR-338-3p is regulated by estrogens through GPER in breast cancer cells and cancer-associated fibroblasts (CAFs). Cells 7, 203.

Wang F., Chen Q., Huang G., Guo X., Li N., Li Y. and Li B. (2018). BKCa participates in E2 inducing endometrial adenocarcinoma by activating MEK/ERK pathway. BMC Cancer 18, 1128.

Wang Z., T. Li T.E., Chen M., Pan J.J. and Shen K.W. (2020). miR-106b-5p contributes to the lung metastasis of breast cancer via targeting CNN1 and regulating Rho/ROCK1 pathway. Aging (Albany NY). 12, 1867-1887.

Yan Y., Liu C., Zhang J., Li W., Yin X., Dong L., Pang S. and Li X. (2021). SMC4 knockdown inhibits malignant biological behaviors of endometrial cancer cells by regulation of FoxO1 activity. Arch. Biochem. Biophys. 712, 109026.

Yang J., Li T., Gao C., Lv X., Liu K., Song H., Xing Y. and Xi T. (2014). FOXO1 3'UTR functions as a ceRNA in repressing the metastases of breast cancer cells via regulating miRNA activity. FEBS Lett. 588, 3218-3224.

Yu Z., Lin X., Tian M. and Chang W. (2018). microRNA-196b promotes cell migration and invasion by targeting FOXP2 in hepatocellular carcinoma. Oncol. Rep. 39, 731-738.

Zembruski N.C.C., Stache V., Haefeli W.E. and Weiss J. (2012). 7-Aminoactinomycin D for apoptosis staining in flow cytometry. Anal. Biochem. 429, 79-81.

Zeng M., Li M., Li M., Zhang B., Li B., Zhang L., Feng W. and Zheng X. (2018). 2-phenylacetamide isolated from the seeds of *Lepidium apetalum* and its estrogen-like effects *in vitro* and *in Vivo*. Molecules 23, 2293.

Zeng Y.B., Liang X.H., Zhang G.X., Jiang N., Zhang T., Huang J.Y., Zhang L. and Zeng X.C. (2016). miRNA-135a promotes hepatocellular carcinoma cell migration and invasion by targeting forkhead box O1. Cancer Cell Int. 16, 63.

Zhang C., Yao C., Li H., Wang G. and He X. (2014). Combined elevation of microRNA-196a and microRNA-196b in sera predicts unfavorable prognosis in patients with osteosarcomas. Int. J. Mol. Sci. 15, 6544-6555.

Zhao J.G., Ren K.M. and Tang J. (2014). Zinc finger protein ZBTB20

promotes cell proliferation in non-small cell lung cancer through repression of FoxO1. FEBS Lett. 588, 4536-4542.

Zhou W.J., Zhang J., Xie F., Wu J.N., Ye J.F., Wang J., Wu K. and Li M.Q. (2021). CD45RO-CD8+ T cell-derived exosomes restrict estrogen-driven endometrial cancer development via the ERβ/miR-765/PLP2/Notch axis. Theranostics 11, 5330-5345.

Accepted December 12, 2022